Simultaneous adsorption of Cd, Cr, Cu, Pb, and Zn by an iron-coated Australian zeolite in batch and fixed-bed column studies

Thuy Chung Nguyen, Paripurnanda Loganathan, Tien Vinh Nguyen, Saravanamuthu Vigneswaran, Jaya Kandasamy, Ravi Naidu

PII: S1385-8947(15)00245-4
DOI: http://dx.doi.org/10.1016/j.cej.2015.02.047
Reference: CEJ 13300

To appear in: *Chemical Engineering Journal*

Received Date: 27 November 2014
Revised Date: 9 February 2015
Accepted Date: 11 February 2015

Please cite this article as: T.C. Nguyen, P. Loganathan, T.V. Nguyen, S. Vigneswaran, J. Kandasamy, R. Naidu, Simultaneous adsorption of Cd, Cr, Cu, Pb, and Zn by an iron-coated Australian zeolite in batch and fixed-bed column studies, *Chemical Engineering Journal* (2015), doi: http://dx.doi.org/10.1016/j.cej.2015.02.047

Simultaneous adsorption of Cd, Cr, Cu, Pb, and Zn by an iron-coated Australian zeolite in batch and fixed-bed column studies

Thuy Chung Nguyen[1], Paripurnanda Loganathan[1], Tien Vinh Nguyen[1], Saravanamuthu Vigneswaran[1]*, Jaya Kandasamy[1], Ravi Naidu[2]

[1]*Faculty of Engineering and Information Technology, University of Technology, Sydney, NSW, 2007, Australia*

[2] *CERAR and CRCCARE, University of South Australia, Adelaide, SA, 5095, Australia*

**corresponding author: s.vigneswaran@uts.edu.au*

Tel: 61 – 2 – 9514 2641

Fax: 61 – 2- 9514 2633

ABSTRACT

Excessive levels of heavy metals in water are an environmental hazard. An Australian zeolite with (ICZ) and without (Z) iron-coating, was used to remove five heavy metals from aqueous solutions using adsorption in batch and column experiments. The batch study showed that the Langmuir adsorption capacities of heavy metals on Z and ICZ at pH 6.5 and ionic strength 10^{-3} M $NaNO_3$ were in the order Pb > Cu > Cd > Cr, Zn for single metal (5.0-11.2 mg/g) and for mixed metals solution (3.7-7.6 mg/g). The data for the kinetics of adsorption satisfactory fitted to both the pseudo-first and second order models with fits slightly better for the latter model. Data fitted to a diffusion model revealed that adsorption took place in two or more than two different stages: a fast external surface adsorption, and a gradual adsorption controlled by both film diffusion and intra-particle diffusion. The column adsorption data were fairly well described by Thomas model, with the order of Thomas adsorption capacity following a similar trend as in the batch study. In both batch and column experiments, the adsorption capacities were higher for ICZ than for Z and were generally lower in mixed metals system than in single metals system. Leaching of used ICZ columns with 0.1 M HCl, resulted in 64-93% of adsorbed metals being desorbed, and 10% of Fe being dissolved from the ICZ.

Keywords: adsorption, heavy metals, iron-coated zeolite, zeolite

1. Introduction

Heavy metals contamination of water bodies presents a significant threat to environment and public health because of their toxicity, accumulation in the food chain and persistence in nature. Strict regulations and guidelines have been imposed or recommended in many countries to restrict heavy metals contamination of natural water bodies [1,2]. There are many chemical and physical processes to remove heavy metals from water. Of these, adsorption is one of the promising technologies due to its high removal efficiency, and simplicity, provided easy availability of low-cost adsorbent can be found locally. Locally available zeolites have been utilised as low-cost adsorbents for the removal of heavy metals in many countries [3-5]. Wang and Peng [5] presented the adsorption capacities of natural zeolites from several countries reported in literature for Cd, Cr, Cu, Co, Mn, Ni, Pb, and Zn. They stated that these information were obtained from adsorption in solutions containing only one metal which may not be directly applicable to real wastewater system where there are several metal ions co-exist and they may compete with each other for adsorption. The difference in adsorption capacities between metals are commonly explained using hydration energy, hydrolysis constant, electro-negativity, and hydroxide solubility product of the metals [6].

Some studies have shown that modification of zeolite surface by coating with iron (ICZ) can enhance the adsorption capacity of the zeolite for heavy metals [7-11]. In batch experiments, Han et al. [8] found that an iron oxide-coated zeolite had greater adsorption capacity than zeolite for Cu. They reported that of the three models used, Thomas model described the adsorption of Cu on the iron oxide-coated zeolite in fixe-bed column the best at all flow rates, initial Cu concentrations, and bed depths. Similarly, Kragović et al. [11] showed that an iron oxide-coated zeolite had higher adsorption capacity than zeolite for Pb. In contrast to the above single-metal adsorption studies, Doula [9] reported that an iron-modified zeolite had higher adsorption capacities than unmodified zeolite for Cu, Zn, and Mn from a solution containing all these metals in batch studies. At high metals concentrations, Mn adsorption by both modified and unmodified zeolite decreased due to competition from Zn and Cu. They also found that Zn adsorption marginally decreased and Cu adsorption was similar to the adsorption pattern of Cu-only solution. The affinity of the metals for both modified and unmodified zeolite followed the order, Cu > Zn > Mn.

Most of the studies using zeolite or ICZ were conducted only in static batch

experiment or on individual metals. Studies using fixed-bed column which are more relevant to real operating systems on natural waters are necessary. Results of batch adsorption studies which are conducted under static condition may sometimes be different from those conducted in dynamic column adsorption system [12]. For example, Baker et al. [3] reported that the metal adsorption capacity for a Jordanian zeolite followed the order Pb > Cd > Cu > Zn but the order in column adsorption system was Cd > Zn > > Pb > Cu. As many metals co-exist in water they can compete with each other for adsorption and therefore it is important to consider the simultaneous removal of co-existing metals. Therefore, the aim of this research was to determine the adsorption behaviour of Cd, Cu, Cr, Pb, and Zn individually and simultaneously on an Australian natural zeolite with and without iron-coating, after their thorough characterisation, in batch and column experiments and determine the mechanisms of adsorption. Desorption of the adsorbed metals and stability of the iron-coatings were also determined. Simultaneous adsorption of several heavy metals in fixed-bed columns and their modelling, and an investigation of the iron-coatings' stability in zeolite during desorption of metals are novel features of this study.

2. Materials and Methods

2.1. Preparation of iron-coated zeolite (ICZ)

The zeolite used in this study was obtained from an Australian natural deposit at Werris Creek, New South Wales and supplied by Escott. Ltd. Company, Australia. The ICZ was prepared by a method similar to that of Doula [9] by mixing 20.0 g of zeolite, 100 mL of freshly prepared 1 M $Fe(NO_3)_3$, and 180 mL of 5 M KOH in a 2 L polyethylene flask. KOH solution was added rapidly to $Fe(NO_3)_3$ with continued stirring. The suspension was diluted to 2 L with deionised water and was held for 60 h in the closed polyethylene flask at 70^{o}C. At the end of this period the reaction vessel was removed from the oven, and the precipitate was centrifuged, washed with distilled water (until free of NO_3^- ions) and then dried. During the 60 h period the suspension was observed to be converted from a red brown colour to a compact red-brown precipitate. This change was explained by Doula [9] to be a conversion of ferrihydrite to geothite.

2.2. Characteristic of the materials

The mineralogy of the zeolite was determined using a XRD Shimadzu S6000 (Japan) diffractometer on powder samples of the zeolite and ICZ. The X-ray diffractometer was equipped with a Cu target operated at 40 kV and 30 mA with a setting of 5–45^{o} (2θ), step time 2^{o}/min. Scanning electron microscopy (SEM), Fourier transform infrared (FTIR) spectroscopy, surface area, and porosity measurements were also conducted on zeolite and ICZ. For the SEM analysis, the samples were imaged, uncoated, in a Zeiss Evo LS15 SEM using its variable pressure mode and an accelerating voltage of 15 kV. FTIR pattern was recorded using a Nicolet 6700 FT-IR Spectrometer equipped with a room temperature DLaTGS detector and a Nicolet FT-IR Smart System with Smart Accessories using a diamond crystal HATR.

Surface area and porosity were determined by nitrogen-sorption measurements carried out at 77 K with a Micromeritics 3 Flex surface characterisation analyser. The BET method was used to calculate the specific surface area. The pore size distribution was derived from the adsorption branch of the isotherm by using the Barrett–Joyner–Halenda (BJH) method.

Samples of zeolite and ICZ were analysed by Energy-dispersive X-ray spectroscopy (EDS). An EDS system called JED-2300/2300F Analysis Station was used to determine the chemical elemental composition.

Zeta potentials were measured on the suspensions of zeolite and ICZ in deionised water at an ionic strength of 10^{-3} M $NaNO_3$ and initial pH ranging from 3.0 to 9.0. The pH adjustment was made utilising 0.1 M NaOH or 0.1 M HNO_3 solutions and the pH was measured using a portable pH meter. The suspensions were agitated in a flat shaker at a shaking speed of 120 rpm at room temperature (25 ± 2^{o}C) for 8 h. At the end of the period, the pH (equilibrium pH) and zeta potential were determined. Zeta potential was measured using a zeta sizer nano instrument (Nano ZS Zen3600, Malvern, UK).

2.3. Chemical analysis

All chemicals used were of analytical reagent grade. Heavy metal nitrates, NaOH, and HNO_3 were supplied by Sigma-Aldrich, Australia (reagent grade) and they were used as received. Stock solutions of Pb, Zn, Cu, Cd and Cr were prepared using $Pb(NO_3)_2$, $Zn(NO_3)_2$ $6H_2O$, $Cu(NO_3)_2$ $5H_2O$, $Cd(NO_3)_2$ $4H_2O$, and $Cr(NO_3)_3$ $9H_2O$, respectively. The initial pH of the test solutions was adjusted to the desired value by using dilute solutions of 0.1 M NaOH

and 0.1 M HNO_3. Heavy metal analyses were made using a Microwave Plasma-Atomic Emission Spectrometer (MP-AES- 4100 Agilent).

2.4. Batch adsorption experiment

2.4.1. Equilibrium experiments

Batch mode experiments on adsorption of heavy metals on zeolite and ICZ from solutions containing single and mixed metals at an initial concentration of 50 mg/L and ionic strength of 10^{-3} $NaNO_3$ was conducted at a temperature of 25 ± 2°C. Zeolite or ICZ were added to 100 mL metal solutions contained in glass bottles to provide adsorbent loading rates of 1.0 to 25.0 g/L. The bottles were sealed and agitated at 120 rpm for 24 h in an orbital shaker. The pH of the suspension was maintained at 6.5 ± 0.2. The suspensions were filtered through a 0.45 µm nylon syringe filter (Cole-Parmer) and heavy metals concentrations were measured using a Microwave Plasma-Atomic Emission Spectrometer (MP-AES- 4100 Agilent). The amount of heavy metal adsorption at equilibrium, q_e (mg/g), was calculated using equation (1),

$$q_e = \frac{(C_o - C_e)V}{M} \qquad (1)$$

where, C_o = initial concentration of heavy metal (mg/L); C_e = equilibrium concentration of the heavy metal (mg/L); V = volume of the solution (L) and M = mass of adsorbent (g). The adsorption experiments were duplicated and the average values were taken for data analysis. The difference between duplicate values was within ± 5 %. The adsorption data were fitted to the Langmuir adsorption isotherm which is described in Table 1.

Table 1

2.4.2. Kinetic experiments

Batch adsorption kinetic experiments were conducted on single and mixed metals solutions at a heavy metal concentration of 5 mg/L each in a set of glass flasks containing 100 mL of heavy metal solution and adsorbent dosage of 2.0 g/L at an ionic strength of 10^{-3} M $NaNO_3$ and pH 6.5. The suspensions were agitated in a flat shaker at 120 rpm for 72 h at room temperature (25 ± 2°C). Aqueous samples were taken at different time intervals and the concentrations of heavy metals were measured. The amounts of heavy metals adsorption at time t, q_t (mg/g), were calculated using an equation similar to equation (1) where C_e was replaced by C_t (mg/L), the concentration of heavy metal at time t (mg/g) and q_e by q_t.

The adsorption data were analysed using pseudo-first and pseudo-second order kinetic models and the intra-particle diffusion model of Weber and Morris [13]. The equations for these models and the methods of calculating the model parameters are presented in Table 1.

2.5. Column adsorption experiments

Fixed-bed columns used in this study were made up of 2.5 cm inner diameter Pyrex glass tube with a stainless steel sieve attached to the bottom of the column, followed by a layer of glass beads in order to provide a uniform flow of the solution through the column. A known quantity (40 g) of the zeolite or ICZ was packed in the column to yield a bed height of 12 cm. Heavy metals solutions containing individual or mixed metals at concentrations of 5 mg/L, each were pumped downward through the column at a filtration velocity of 0.52 m/h (8 mL/min) to yield a bed volume of 0.038 L and an empty bed contact time of 11.5 min, controlled by a peristaltic pump. The effluents at the outlet of the column were collected at regular time intervals and the heavy metals concentrations were measured using a Microwave Plasma-Atomic Emission Spectrometer (MP-AES- 4100 Agilent).

2.6. Column desorption experiments

Metals adsorbed onto the ICZ need to be desorbed before using the ICZ again to remove heavy metals. An experiment was conducted by desorbing the previously adsorbed heavy metals (see section 2.5) by passing 0.1 M HCl at a velocity of 0.52 m/h through ICZ and zeolite columns. The concentrations of the desorbed metals and Fe dissolved from the adsorbents in the column leachate were measured periodically for 40 bed volumes (160

mins). 0.1 M HCl served to desorb the metals because adsorption of metals is low at very acidic conditions [2,6]. Han et al. [8] successfully used 1 M HCl to regenerate an iron oxide-coated zeolite after its exhaustion with adsorption of Cu. Fe concentration in the leachate was measured to determine the stability of the Fe coatings in the zeolite.

3. Results and discussion

3.1. Characteristics of materials

The XRD and FTIR patterns of ICZ were similar to those of zeolite and therefore only patterns of zeolite are presented (Figure 1 and 2). The XRD spectra of zeolite showed that the zeolite comprised primarily of heulandite (2θ: 10.0^o, 19.0^o, 22.7^o, 30.0^o) [14,15] and small amount of quartz (2θ: 21.0^o, 27.0^o, 36.5^o) [16,17] (Figure 1). X-ray diffractograms of ICZ revealed no notable change in the basic zeolite diffraction peaks, indicating no detectable damage to the zeolite framework, or the presence of additional Fe oxidic or oxo-hydroxidic crystalline phases resulting from the iron oxide coating of the zeolite. However, XRD cannot detect any amorphous Fe species that may have formed on the zeolite surface.

Figure 1 and Figure 2

Figure 2 shows the FTIR spectra for zeolite. The peak at 1048 cm^{-1} is attributed to asymmetric O–T–O stretching vibration (vO-T-O) where T represent Si or Al [18]. The peak at 462 cm^{-1} is probably from the bending of the bonds inside TO_4 [19]. The peaks at 3447 cm^{-1} and 1638 cm^{-1} can be assigned to the stretching vibration mode of lattice water and hydroxyl groups and OH bending vibration mode of adsorbed water molecules [20].

The surface area (BET) of zeolite and ICZ were 15.4 g/m^2 and 7.51 g/m^2, respectively. The lower surface area of ICZ compared to zeolite is probably due to the blockage of the pores in zeolite by the iron oxide coatings. EDS data showed that the Fe content of ICZ was 8.46% while that of zeolite was only 1.03 % (Figure 3).

Figure 3

A distinct difference in the surface morphology of zeolite and ICZ can be observed in the SEM photographs (Figure 4). The coated zeolite surfaces were apparently occupied by clusters of newborn iron oxides, which were formed during the iron oxide coating process.

Figure 4

The negative zeta potentials of zeolite at all pHs (pH 3.0 to 9.0) were higher than those of ICZ (Figure 5). The zero point of charge (ZPC, pH at which the net surface charge on the particle is zero) of zeolite was approximately pH 2.2 whereas that of ICZ was nearly pH 5.6. This shows that more negative charges were available in zeolite than in ICZ. Therefore, zeolite can potentially adsorb larger amounts of the positively charged heavy metal cations than ICZ by outer-sphere complexation through electrostatic attraction (coulombic forces).

Figure 5

3.2. Batch experiment

3.2.1. Batch equilibrium adsorption modelling

The adsorption isotherms for individual and mixed metals showed that the adsorption capacity decreased in the following order for both zeolite and ICZ: Pb > Cu > Cd > Zn, Cr (Figure 6 and 7) and the adsorption of the metals capacities on ICZ was higher than those on zeolite. The data for the adsorption of all metals from single metal solution as well as from the mixed metals solution satisfactorily fitted to the Langmuir adsorption model. This suggests that the adsorption sites were homogeneous with monolayer adsorption coverage. However, the fits were better for single metal solutions (R^2 = 0.937-0.992) than for mixed metals solution (R^2 = 0.743-0.951) probably because of competition for adsorption between

metals in the mixed metals solution (Table 2). Competition for adsorption of metals is reflected in the lower Langmuir adsorption capacity for each metal in mixed metals system than in single metal system. The data fits to two other adsorption models, i.e. Freundlich (single metal solution, R^2 = 0.905-0.985; mixed metals solution, R^2 = 0.450-0.876) and Dubinin-Radushkevich models [21] (single metal solution, R^2 = 0.526-0.870; mixed metals solution, R^2 = 0.682-0.971) [Supplementary tables ST1 and ST2] were less satisfactory than the Langmuir model fits.

Figure 6 and Figure 7

Table 2

The adsorption capacities of zeolite (Table 2) are comparable to those reported for zeolites from other countries. For example, a zeolite from Greece had Langmuir adsorption capacities (mg/g) of 3.5, 4.1, 4.6, and 5.9 for Zn, Cr, Cd, and Cu, respectively [22]. Another study done in South Korea revealed that a zeolite had Langmuir adsorption capacities (mg/g) of 6.5, 7.1, and 8.9 for Cu, Cd, and Pb, respectively [10]. The adsorption capacities of ICZ (Table 2) are higher than those of zeolites and many other low-cost adsorbents. For example, Mishra and Patel [23] reported Langmuir adsorption capacity values (mg/g) of 4.5, 5.0, 5.5, and 7.6 for Pb adsorption at pH 6.0 on kaolin, fly ash, blast furnace slag, and bentonite, respectively. The corresponding values for Zn were 3.1, 5.8, 3.3, and 9.1, respectively. The values reported for Cr and Pb adsorption on fly ash in another study at pH 5 and 6 were 4.4 and 2.5 mg/g, respectively [24]. However, the adsorption capacities of ICZ are lower than those of nano-sized metal oxides, carbon nanotubes and commercial ion exchangers [25-27]. Nevertheless, the advantages of zeolite and ICZ over the other adsorbents are their low cost and their ability to be conveniently used directly in fixed-bed columns, because they have larger particles and better physical stability.

The Langmuir maximum adsorption capacity order for the metals in the single metal and mixed metals systems was Pb > Cu > Cd > Zn, Cr. The adsorption capacities for all metals except for Cr were higher for ICZ than for zeolite on both single metal and mixed metals system. Doula [9] also reported that the adsorption of Cu was higher than Zn on a

zeolite and a Fe-modified zeolite in single and mixed metals systems. For both metals the adsorption of Fe-modified zeolite was higher than that of zeolite.

The reason for ICZ having higher adsorption capacities than zeolite, despite the higher ZPC of the former, is that ICZ has iron oxide which specifically adsorbs heavy metals [1]. The mechanism of adsorbing heavy metals on zeolite is predominantly outer-sphere complexation (non-specific adsorption) via the ion exchange process where the counter balanced alkali and alkalai earth metal ions, Ca^{2+}, Mg^{2+}, Na+, and K+ in the exchangeable sites on zeolite are replaced by heavy metal ions [7]. Some heavy metal ions can also adsorb onto the terminal Al-OH and Si-OH surface sites by inner-sphere complexation (specific adsorption) by releasing protons (H^+) [7, 28]. In the case of ICZ the presence of iron oxides on the zeolite surface would have further increased the adsorption of heavy metals by inner-sphere complexation due to abundant Fe-OH sites in the iron oxides. Strong affinity of iron oxides to heavy metals has been documented in many studies [29]. At high pH (pH 6-7, depending on the metal) the removal of large amounts of heavy metals is due to adsorption of metal hydroxide (MOH^+, where M represents metal) species from solution and surface precipitation of metal hydroxide [1]. Metal hydroxide species have higher affinity than divalent metal ions for adsorption on aluminosilicate and metal oxide surfaces.

The order of the adsorption capacities of the metals (Pb > Cu > Cd > Zn and Cr) can be explained by the first hydrolysis constant of the metals (MOH^+ formation) and solubility product of the metal hydroxides. The lower the first hydrolysis constant, the greater the proportion of MOH^+ which has stronger adsorption than M^{2+} among the various metal species in solution. High solubility product favours precipitation of metals, especially on the surface of adsorbents which can occur at a pH lower than the pH of precipitation in solutions [1]. Lead hydroxide has the highest solubility product and lowest first hydrolysis constant; consequently it had the highest adsorption capacity [25]. The second metal which had the highest adsorption capacity was Cu. The reason for this is that it has the second highest solubility product and second lowest hydrolysis constant [25].

3.2.2. Batch adsorption kinetics modelling

Adsorption of all metals from single metal and mixed metals solutions on both zeolite and ICZ increased with time and reached equilibrium only at approximately 20 h. The kinetic

adsorption data fitted satisfactorily to both pseudo-first and pseudo-second order models for both single and mixed metals system (Table 3 and 4). The models predicted equilibrium adsorption capacities were approximately equal to the corresponding experimental values for both models. When the R^2 values were considered, however, the pseudo-second order model appeared to fit the data better than the pseudo-first order model. The better fit of the pseudo-second order model suggests that chemical process may be the rate-limiting step in the adsorption [20].

The intra-particle diffusion model plot of the data is shown in Figure 8. According to Weber and Morris [13], if intra-particle diffusion occurs the plot would be linear and if the plot passes through the origin then the rate limiting process is only the intra-particle diffusion. The data, however, exhibited two or more linear portions (Figure 8). The first linear portion up to 4 h was a fast step which can be attributed to heavy metal transport by film diffusion and adsorption on the external surfaces. This is followed by a slow step where intra-particle diffusion of heavy metal through the pores and channels of the adsorbent occurs which is represented by the second straight line. As the entire plot was not linear and did not pass through the origin, both film diffusion and intra-particle diffusion appeared to have occurred simultaneously during the adsorption process. The third step which occurred beyond 16 h was the equilibrium stage where the adsorption sites were saturated and the intra-particle diffusion process was nearly completed.

Figure 8

Table 3 and 4

3.3. Fixed-bed column experiments

3.3.1 Breakthrough curves and modelling

Adsorption of single and mixed heavy metals by zeolite and ICZ is presented in the form of breakthrough curves (Figures 9 and 10). The heavy metals breakthrough generally occurred faster and the breakthrough curve was steeper for Cr and Zn than the other metals. The time to reach the plateau of C_t/C_o was significantly higher for Pb than Cd, Cu, Zn and Cr. The breakthrough was slowest and the breakthrough curve was least steep for Pb. Jeon et al.

[10] reported similar results for a zeolite and an iron-coated zeolite removing Cd, Cu, and Pb in column experiments where the breakthrough was not very different between Cu and Cd. However, there was no breakthrough for Pb when up to 800 bed volumes were tested. It is hypothesised that Pb was removed in greater quantities, compared to other metals, because of its solution chemistry which was discussed under batch adsorption results. The order of column adsorption capacities calculated from the breakthrough curves (Pb > Cd, Cu > Zn > Cr) agreed fairly well with that obtained from the batch adsorption experiments (Table 5). Furthermore, the metals removal efficiencies were higher for ICZ (1.17-2.28 mg/g for the single metal system and 0.76-1.03 mg/g for the mixed metals system) than for zeolite (0.81-1.67 mg/g for the single metal system and 0.35-0.63 mg/g for the mixed metals system) as observed in the batch adsorption study. ICZ had higher removal efficiencies because of the presence of iron oxides.

The Thomas model satisfactorily described the breakthrough behaviour of the different heavy metals in both zeolite and ICZ (R^2 = 0.876-0.959) (Table 5). The model predicted adsorption capacities (q_o) were approximately the same as the corresponding adsorption capacities calculated from the breakthrough curves. For all metals, the q_o values were higher for single than mixed metals system reflecting the competition for adsorption between metals in the later system.

Although the column adsorption capacities calculated from the breakthrough curves and Thomas model predicted adsorption capacities (Table 5) followed the same order as the batch Langmuir adsorption capacities (Table 2) for the different metals, the former were much lower than the latter. This is probably due to two reasons. Firstly, the metals flowing through the columns have not reached equilibrium unlike in the batch equilibrium experiment. Secondly, the column adsorption was determined at a lower influent solution metals concentration than the metals concentrations at which Langmuir adsorption maxima were determined.

Figures 9 and 10

Table 5

3.3.2. Desorption of metals and regeneration of zeolite and ICZ

Desorption of metals previously adsorbed on zeolite and ICZ columns by elution with 0.1 M HCl removed 62-90% and 58-85% of adsorbed metals on zeolite in the first and second cycles of adsorption/desorption, respectively (Table 6). The corresponding values for ICZ were 64-93% and 49-85%, respectively. Desorption peaked at around 10-15 bed volumes (40-60 min) and was completed in less than 40 bed volumes (Supplementary Figure 1, SF 1). Despite a large percentage of adsorbed metals being desorbed, the adsorption capacities declined in the second cycle, particularly for ICZ. Han et al. [8] reported that the adsorption capacity of an iron oxide-coated zeolite for Cu decreased in the second cycle after desorption of Cu by 1 M HCl. The reason for the higher reduction in adsorption capacities of ICZ compared to zeolite is probably because some iron oxide coatings in ICZ dissolved in the acidic condition of 0.1 M HCl. The Fe concentration in the leachate from the ICZ column was about 80 times higher compared to that in zeolite (Table 6). Fe dissolved from the iron coatings in the first cycle was 10% of Fe originally present in ICZ (Fe content in ICZ = 8%, total Fe in desorbed solution = 0.081 mg/g ICZ). In comparison, Fe dissolved in the second cycle was much lower (0.75%). Although the regeneration of ICZ reduced the adsorption capacity, partly because of the iron coatings being dissolved, the adsorption capacity of the regenerated ICZ was still higher than that of the original zeolite.

4. Conclusions

Iron oxide coating of an Australian zeolite (ICZ) increased the heavy metal adsorption capacity compared to natural zeolite in both batch and column adsorption experiments whether adsorption was from individual or mixed metals solution. The adsorption reaction can be satisfactorily described by both the pseudo-first-order and the pseudo-second-order kinetic models with the data fit slightly better for the latter model, suggesting a chemical adsorption. Data fit to a diffusion model suggested that adsorption was also governed by intra-particle diffusion. The Langmuir adsorption capacity of the metals for both ICZ and Z at pH 6.5 was Pb > Cu > Cd > Cr, Zn. The column adsorption capacity followed the order of Pb > Cd > Cu > Zn > Cr as calculated from the breakthrough curves as well as using Thomas model. In the mixed metals adsorption the adsorption capacity decreased at high concentrations of metals probably due to competition between metals for adsorption. Overall, both zeolite and ICZ displayed a high affinity for Pb, Cd and Cu, but were less effective at

removing Zn and Cr. Leaching of used ICZ and zeolite columns with 0.1 M HCl, desorbed a large percentage of the adsorbed metals and dissolved 10% Fe from the ICZ. However, the adsorption capacities fell in the second adsorption/desorption cycle, more so for ICZ, probably due to the dissolution of some iron coatings in the acidic conditions of HCl.

Acknowledgements

This study was funded by Cooperative Research Centre for Contamination Assessment and Remediation of the Environment (CRC CARE) (project number 02-050-07).

References

1. P. Loganathan, S. Vigneswaran, J. Kandasamy, R. Naidu, Cadmium sorption and desorption in soils: A review, Crit. Rev. Environ. Sci. Technol. 42 (2012) 489–533.
2. V.K. Gupta, I. Ali, Environmental water: advances in treatment, remediation and recycling. Elsevier Book, Newnes, 2013.
3. H.M. Baker, A.M. Massadeh, H.A. Younes, Natural Jordanian zeolite: removal of heavy metal ions from water samples using column and batch method, Environ. Monit. Assess. 157 (2009) 319–330.
4. M. Hamidpour, M. Kalbasi, M. Afyuni, H. Shariatmadari, P.E. Holm, H.C.B. Hansen, Sorption hysteresis of Cd(II) and Pb(II) on natural zeolite and bentonite, J. Hazard. Mater. 181 (2010) 686–691.
5. S. Wang, Y. Peng, Natural zeolites as effective adsorbents in water and wastewater treatment, Chem. Eng. J. 156 (2010) 11-24.
6. M. Minceva, R. Fajgar, L. Markovska, V. Meshko, Comparative study of Zn^{2+}, Cd^{2+}, and Pb^{2+} removal from water solution using natural clinoptilolitic zeolite and commercial granulated activated carbon. Equilibrium of adsorption, Sep. Sci. Technol. 43 (2008) 2117-2143.
7. A. Dimirkou, M.K. Doula, Use of clinoptilolite and Fe-overexchanged clinoptilolite in Zn^{2+} and Mn^{2+} removal from drinking water, Desalination 224 (2008) 280–292.
8. R. Han, L. Zou, X. Zhao, Y. Xua, F. Xua, Y. Li, Y. Wang, Characterization and properties of iron oxide-coated zeolite as adsorbent for removal of copper(II) from solution in fixed bed column, Chem. Eng. J. 149 (2009) 123–131.
9. M.K. Doula, Simultaneous removal of Cu, Mn and Zn from drinking water with the use of clinoptilolite and its Fe-modified form, Water Res. 43 (2009) 3659–3672.
10. C.S. Jeon, S.W. Park, K. Baek, J.S. Yang, J.G. Park, Application of iron-coated zeolites (ICZ) for mine drainage treatment, Korean J. Chem. Eng. 29 (2012) 1171–1177.
11. M. Kragovic, A. Dakovic, Z. Sekulic, M. Trgo, M. Ugrina, J. Peric, G.D. Gatta, Removal of lead from aqueous solutions by using the natural and Fe(III)- modified zeolite, Appl. Surf. Sci. 258 (2012) 3667–3673.
12. P. Loganathan, S. Vigneswaran, J. Kandasamy, N.S. Bolan, Removal and recovery of phosphate from water using sorption, Crit. Rev. Environ. Sci. Technol. 44 (2014) 847-907.

13. W.J. Weber, S.C. Morris Jr, Intraparticle diffusion during the sorption of surfactants onto activated carbon, J. Sanit. Eng. Div. Am. Soc. Civ. Eng. 89 (1963) 53-61.
14. M.M.J. Treacy, J.B. Higgins, Collection of simulated XRD powder patterns for zeolites, fifth ed., Elsevier, 2007.
15. V.P. Deshpande, B.T. Bhoskar, Characterization and dielectric study of zeolite Zsm5, Inter. J. Eng. Res. Technol. 1 (2012). ESRSA Publications.
16. W. Mozgawa, The influence of some heavy metals cations on the FTIR spectra of zeolites, J. Mol. Struct. 555 (2000) 299–304.
17. T.S. Jamil, H.S. Ibrahim, I.H. Abd El-Maksoud, S.T. El-Wakeel, Application of zeolite prepared from Egyptian kaolin for removal of heavy metals: I. Optimum conditions, Desalination, 258 (2010) 34-40.
18. M.K. Doula, A. Ioannou, A. Dimirkou, Copper adsorption and Si, Al, Ca, Mg, and Na release from clinoptilolite, J. Colloid Interf. Sci. 245 (2002) 237–250.
19. M.K. Doula, Synthesis of a clinoptilolite–Fe system with high Cu sorption capacity, Chemosphere 67 (2007) 731–740.
20. T. Nur, P. Loganathan, T.C. Nguyen, S. Vigneswaran, G. Singh, J. Kandasamy, Batch and column adsorption and desorption of fluoride using hydrous ferric oxide: Solution chemistry and modelling, Chem. Eng. J. 247 (2014) 93–102.
21. M. Karthikeyan, K.K. Satheeshkumar, K.P. Elango, Removal of fluoride ions from aqueous solution by conducting polypyrrole, J. Hazard. Mater. 167 (2009) 300-305.
22. E. Álvarez-Ayusoa, A. García-Sáncheza, X. Querol, Purification of metal electroplating waste waters using zeolites, Water Res. 37 (2003) 4855–4862.
23. P.C. Mishra, R.K. Patel, Removal of lead and zinc ions from water by low cost adsorbents, J. Hazard. Mater. 168 (2009) 319-325.
24. V.K. Gupta, I. Ali, Removal of lead and chromium from wastewater using bagasse fly ash- a sugar industry waste, J. Colloid Interf. Sci. 271 (2004) 321–328.
25. D.P. Sounthararajah, P. Loganathan, J. Kandasamy, S. Vigneswaran, Adsorptive removal of heavy metals from water using sodium titanate nanofibres loaded onto GAC in fixed-bed columns, J. Hazard. Mater. 287 (2015) 306-316.
26. M. Hua, S. Zhang, B. Pan, W. Zhang, L. Lv, Q. Zhang, Heavy metal removal from water/wastewater by nanosized metal oxides: A review, J. Hazard. Mater. 211–212 (2012) 317-331.
27. G.P. Rao, C. Lu, F. Su, Sorption of divalent metal ions from aqueous solution by carbon nanotubes: A review, Sep. Purif. Technol. 58 (2007) 224-231.

28. W. Qiu, Y. Zheng, Removal of lead, copper, nickel, cobalt, and zinc from water by a cancrinite-type zeolite synthesized from fly ash, Chem. Eng. J. 45 (2009) 483–488.
29. M.B. McBride, Reactions controlling heavy metal solubility in soils, Adv. Soil Sci. 10 (1989) 1-56.

Figures captions

Figure 1. XRD patterns of zeolite and ICZ

Figure 2. FTIR spectra of zeolite and ICZ

Figure 3. EDS results of (a) zeolite and (b) ICZ

Figure 4. SEM images of zeolite (left) and ICZ (right) at 40.000 X magnification

Figure 5. Zeta potential of zeolite and ICZ suspensions at an ionic strength 10^{-3} M $NaNO_3$

Figure 6. Batch adsorption isotherms for individual metals on zeolite and ICZ at ionic strength 10^{-3} M $NaNO_3$ and pH 6.5

Figure 7. Batch adsorption isotherms for metals mixture on zeolite and ICZ at ionic strength 10^{-3} M $NaNO_3$ and pH 6.5

Figure 8. Intra-particle diffusion model fit to adsorption data

Figure 9. Breakthrough curves of column experiments for individual metals at pH 6.5

Figure 10. Breakthrough curves of column experiments for metals mixture at pH 5.0

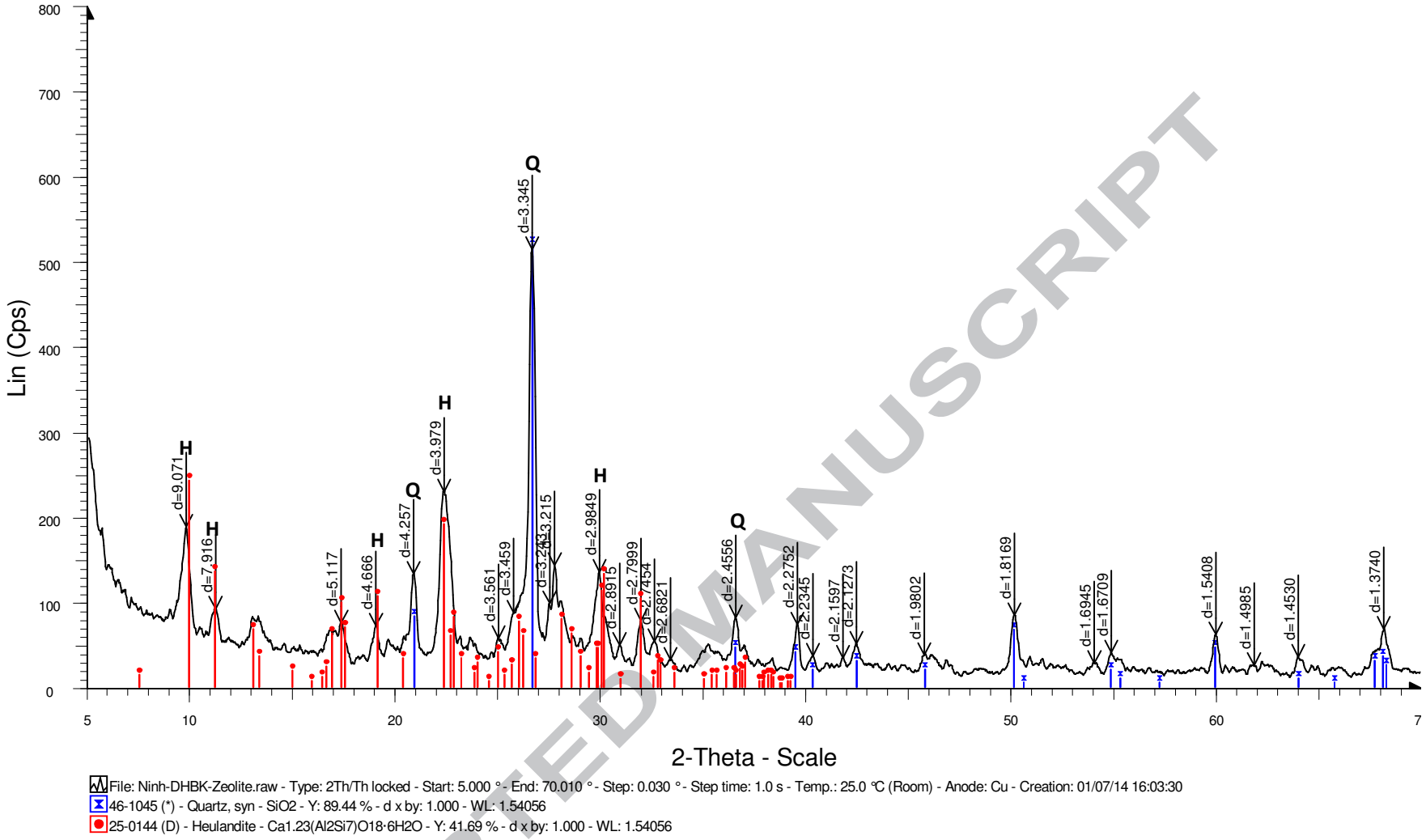

Fig. 1.

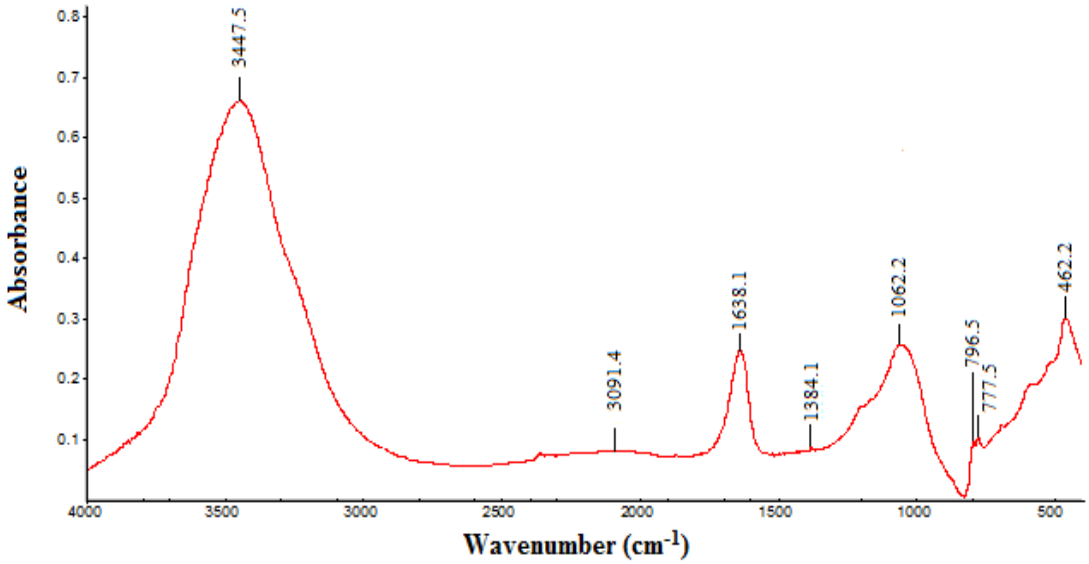

Fig. 2.

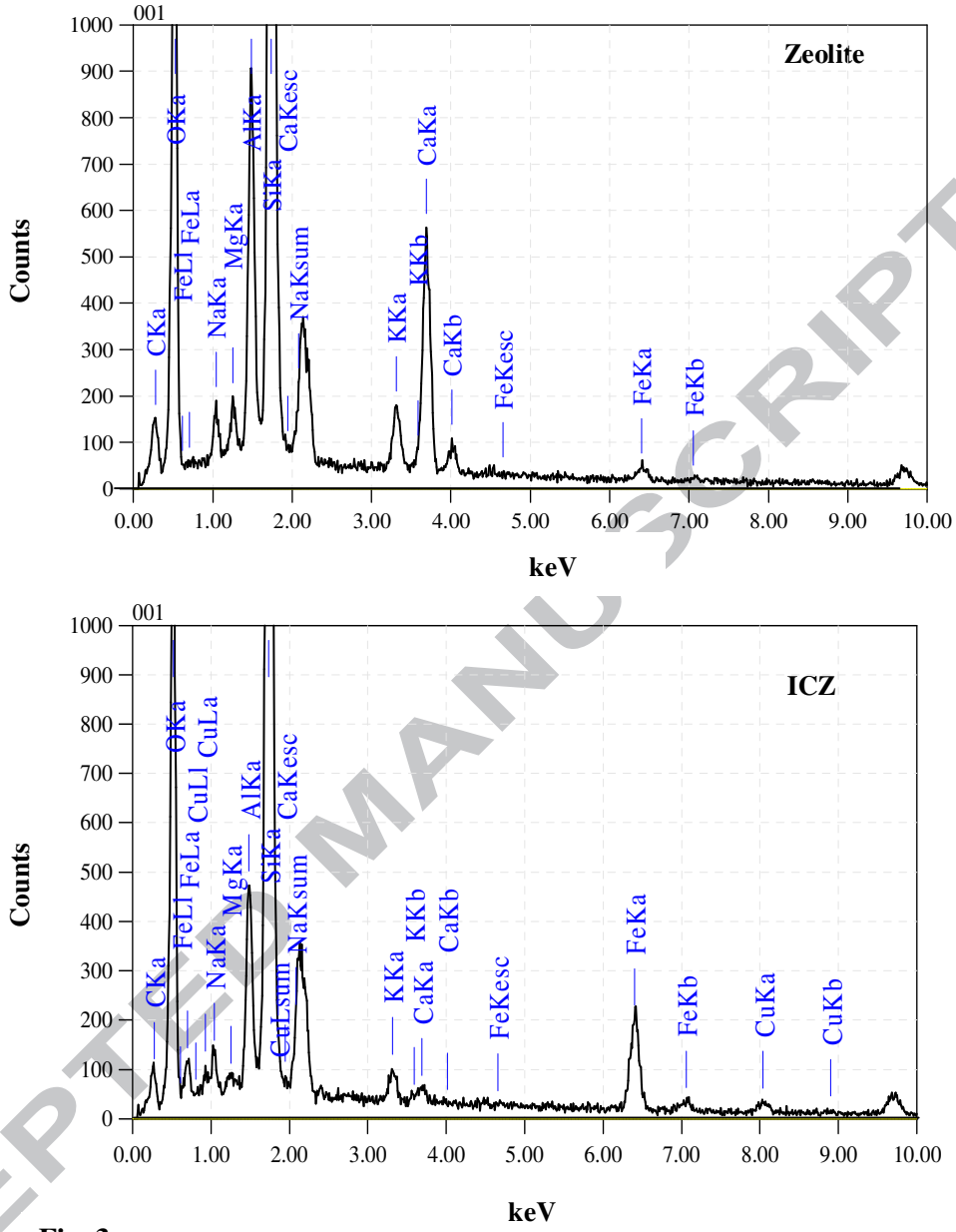

Fig. 3.

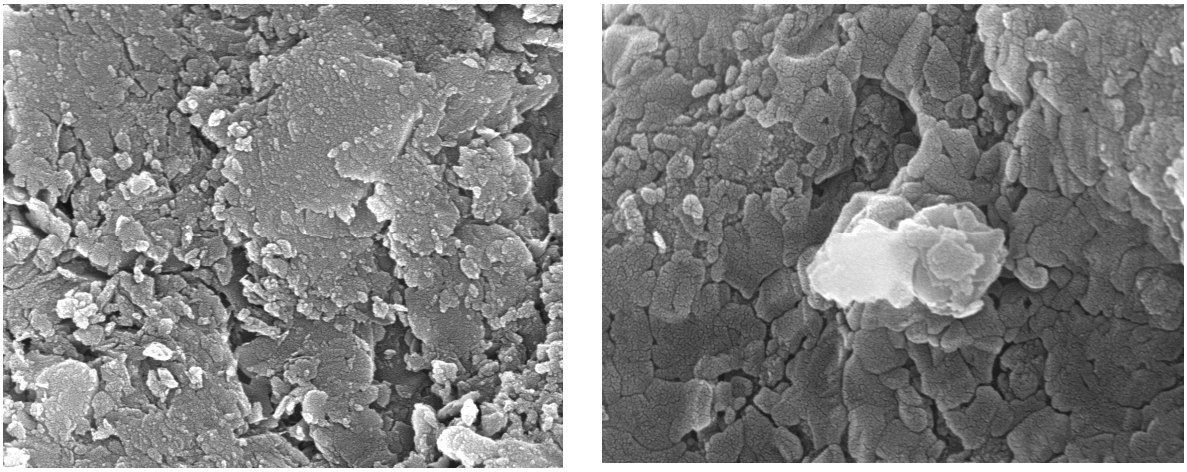

Fig.4.

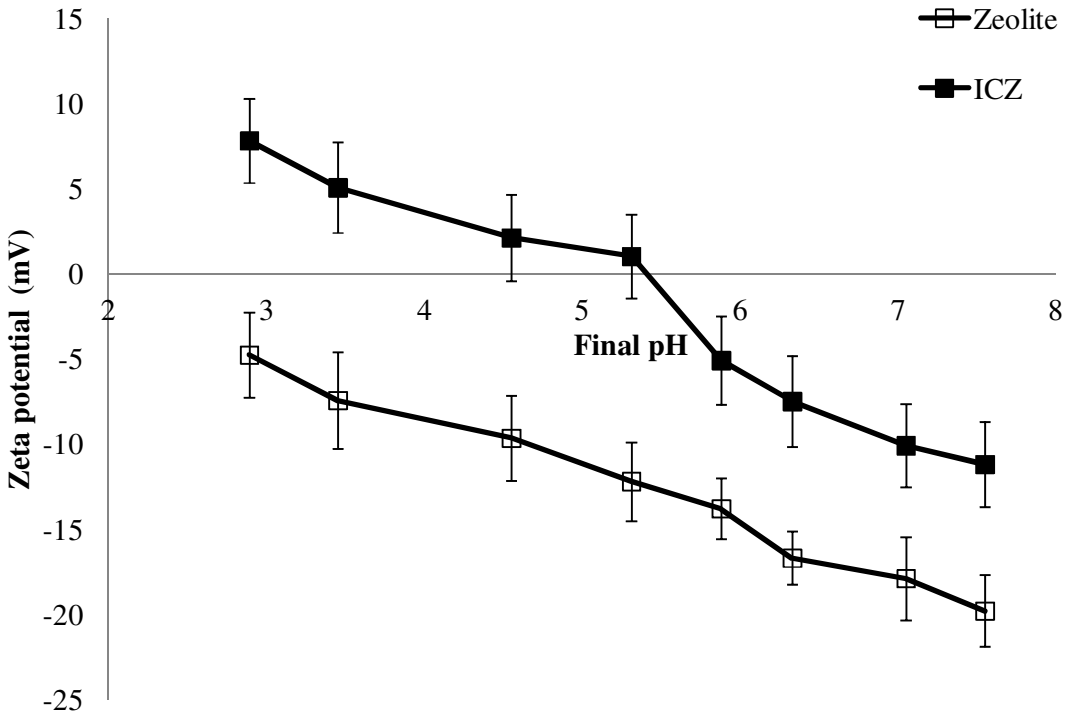

Fig. 5.

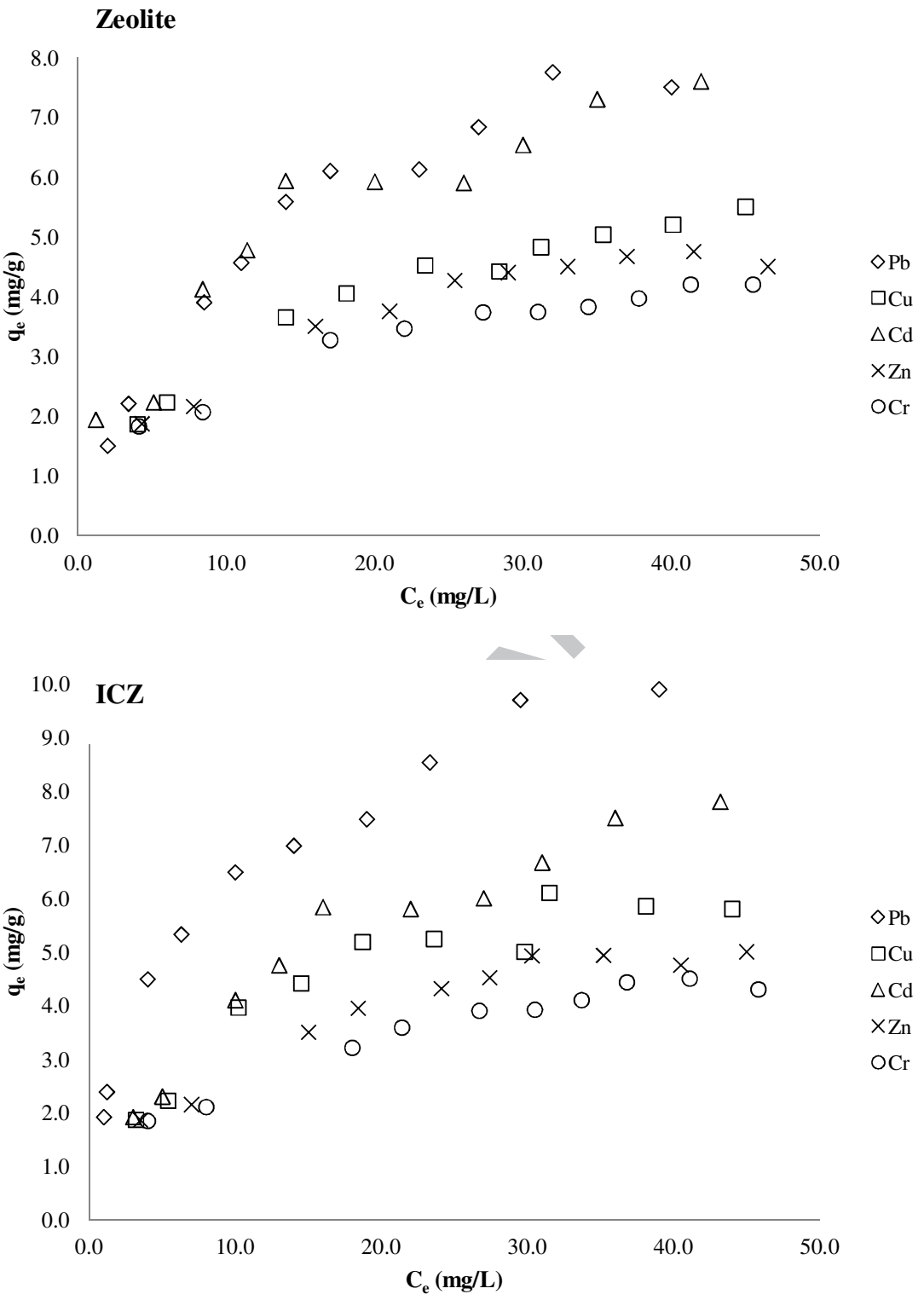

Fig. 6.

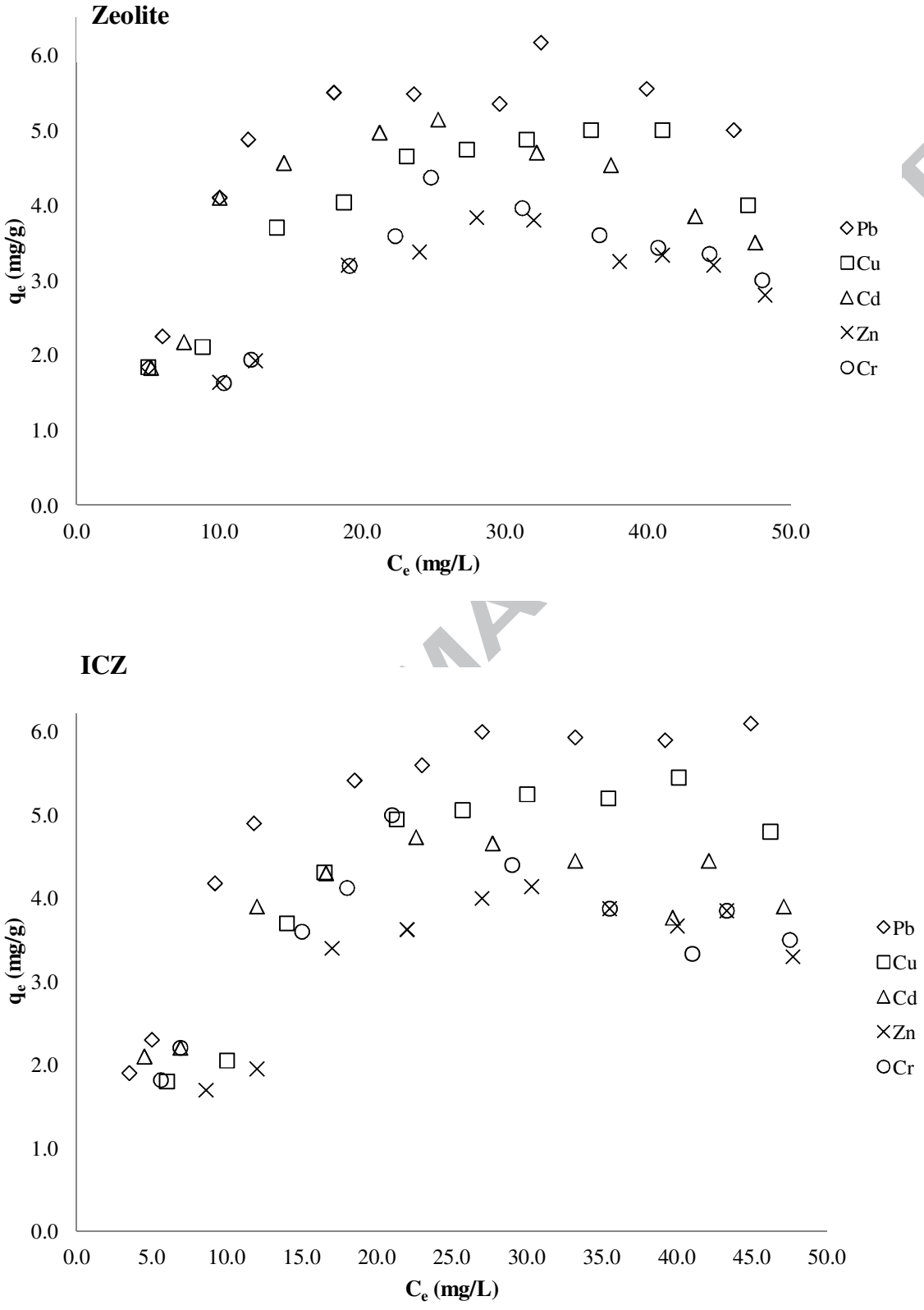

Fig. 7.

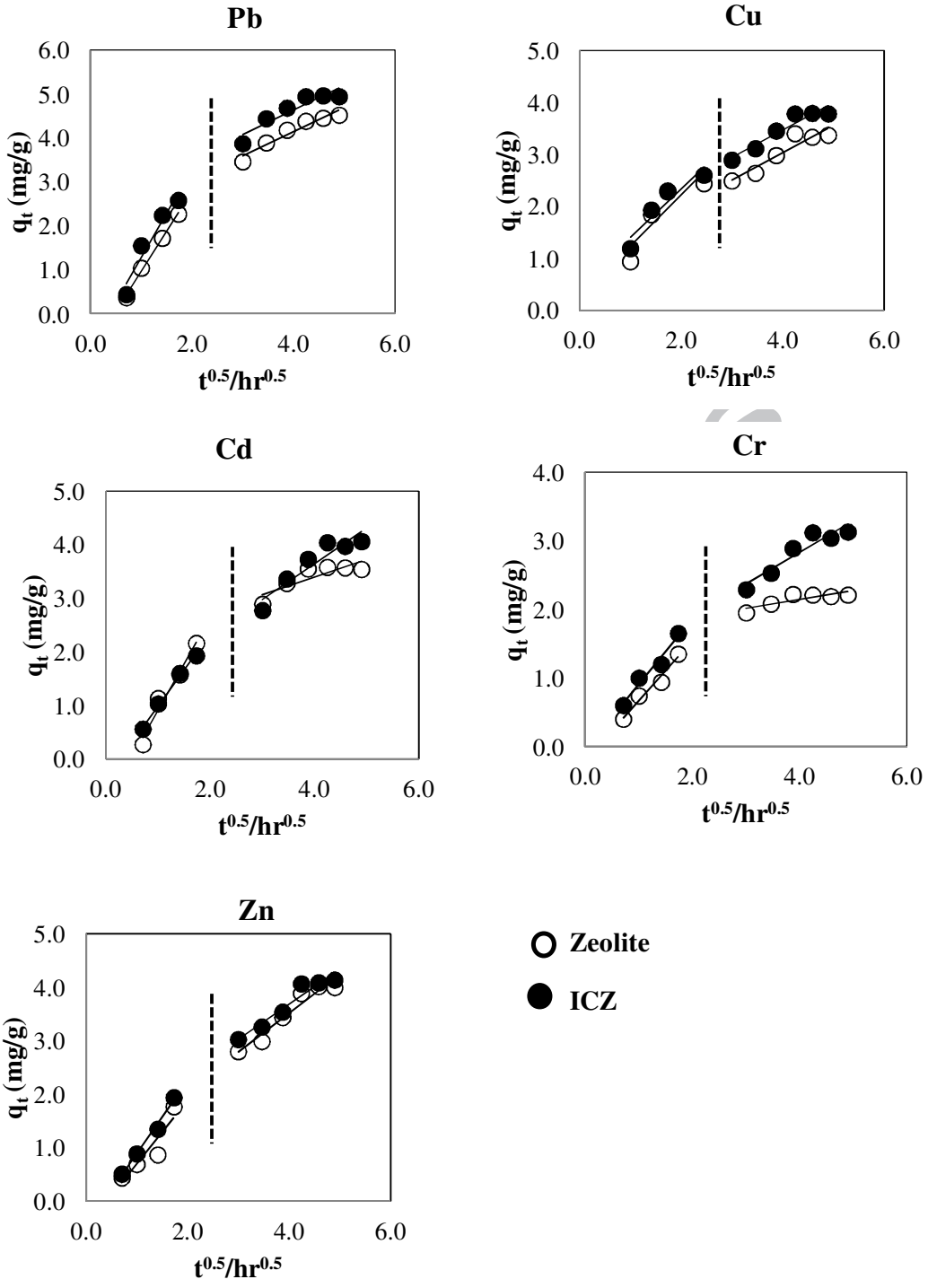

Fig. 8.

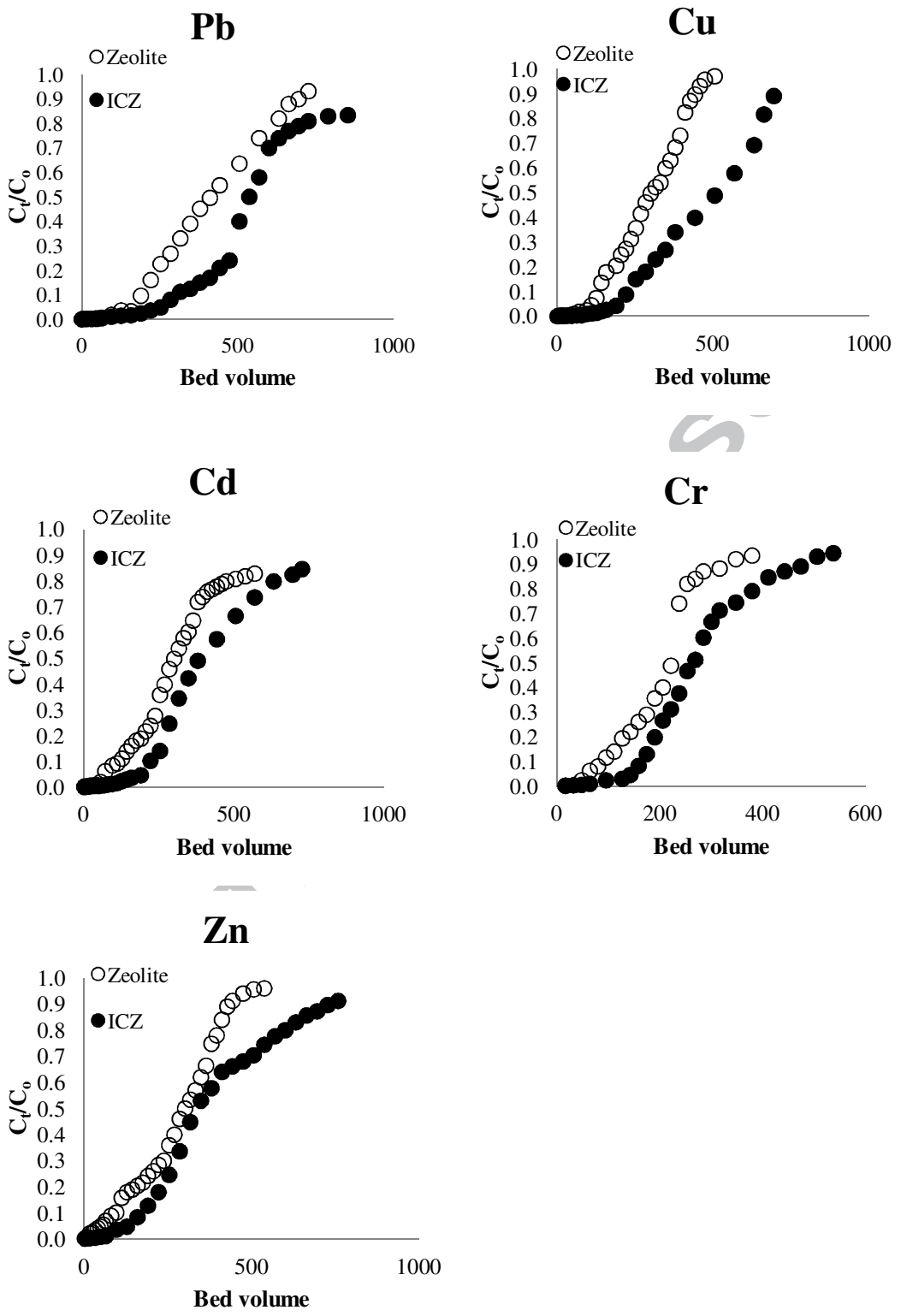
Pb
Zeolite
ICZ
C_t/C_o
Bed volume
Cu
Zeolite
ICZ
C_t/C_o
Bed volume
Cd
Zeolite
ICZ
C_t/C_o
Bed volume
Cr
Zeolite
ICZ
C_t/C_o
Bed volume
Zn
Zeolite
ICZ
C_t/C_o
Bed volume

Fig. 9.

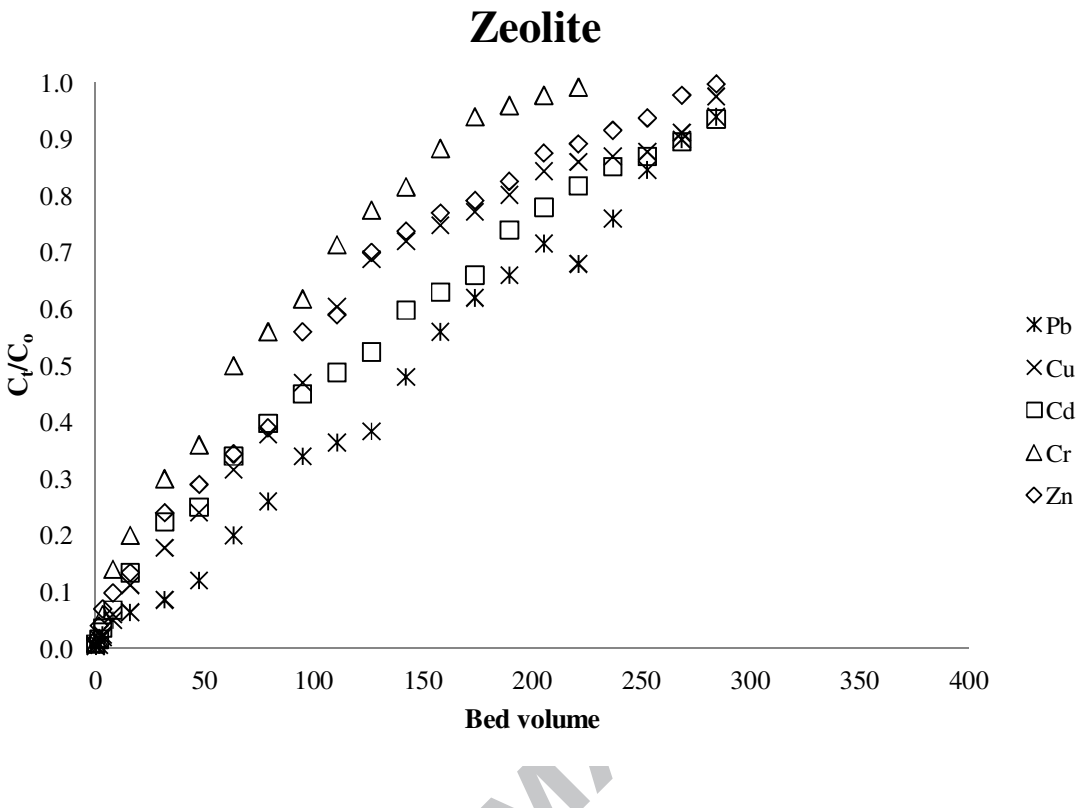

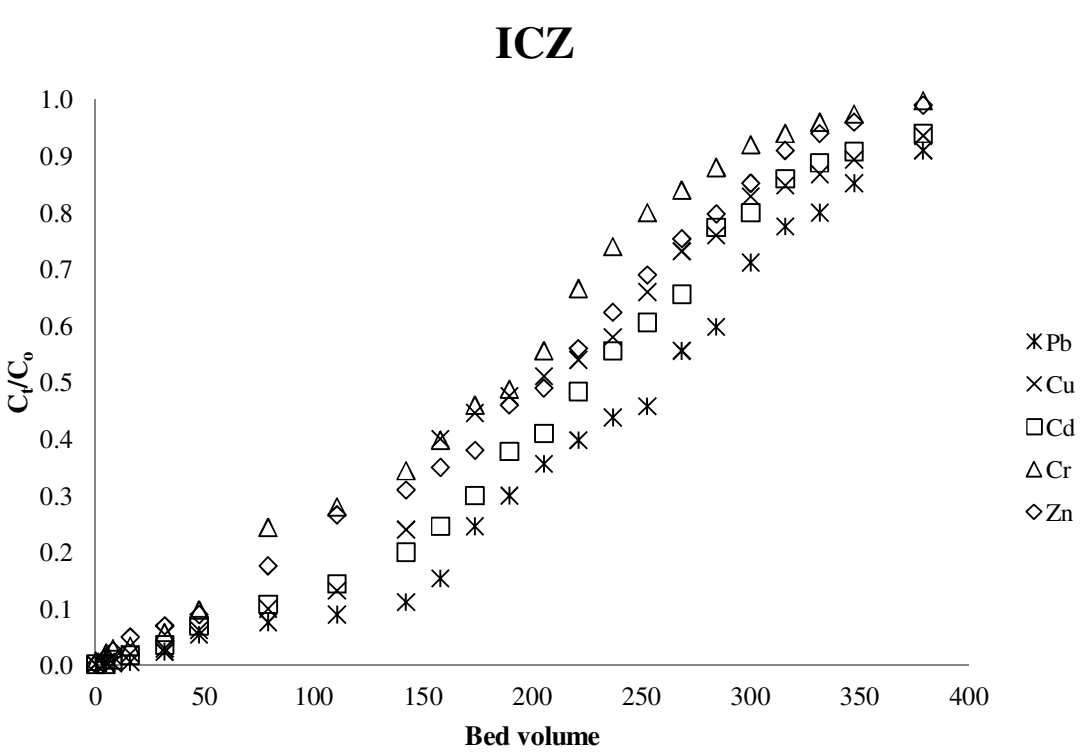

Fig. 10.

Table 1.

The models and equations used for the description of batch and column adsorption of heavy metals (HM) by zeolite and ICZ

Method	Model	Equation	Graphical method used to calculate model constant
Batch	Langmuir	$q_e = \frac{q_{max} K_L C_e}{1 + K_L C_e}$	$\frac{C_e}{q_e} = \frac{1}{q_{max} K_L} + \frac{C_e}{q_{max}}$
		C_e = equilibrium concentration of HM (mg/L), C_e = equilibrium concentration of HM (mg/L), q_e = amount of HM adsorbed (mg/g), q_{max} = maximum amount of HM adsorbed (mg/g); K_L = Langmuir constant related to the energy of adsorption (L/mg)	
	Pseudo-first order kinetic	$\frac{dq_t}{dt} = k_1(q_e - q_t)$	$\ln (q_e - q_{t)} = \ln q_e - k_1 t$
		q_e = amount of HM adsorbed at equilibrium (mg/g); q_t = amount of HM adsorbed at time, t (min) (mg/g) and k_1 = equilibrium rate constant of pseudo-first order sorption (1/min)	
	Pseudo-second order kinetic	$\frac{dq_t}{dt} = k_2(q_e - q_t)^2$	$\frac{t}{q_t} = \frac{1}{k_2 q_e^2} + \frac{t}{q_e}$
		q_e = amount of HM adsorbed at equilibrium (mg/g); q_t = amount of HM adsorbed at time, t (min) (mg/g) and k_2 = equilibrium rate constant of pseudo-second order (1/min)	
	Weber and Morris	$q_t = k_p t^{0.5} + C$	
		q_t = amount of HMs adsorbed at time t (min) (mg/g); k_p = intra-particle diffusion rate constant; C = a constant	
Column	Thomas	$\ln(C_o/C_t - 1) = k_{Th} q_0 M/Q - k_{Th} C_o t$	
		k_{Th} = Thomas rate constant (mL/min mg), q_o= column adsorption capacity (mg/g), C_0 = inlet HM concentration (mg/L), C_t= outlet HM concentration at time t (mg/L), M = mass of adsorbent (g), Q = filtration velocity (mL/min) and t = filtration time (min)	

Table 2.

Langmuir adsorption isotherm parameters for heavy metals (HM) adsorption on zeolite and ICZ at pH 6.5 and ionic strength 10^{-3} M $NaNO_3$ (n= the number of data points)

	HM	Individual metal (C_e = 0 – 50 mg/L)				Metals mixture (C_e = 0 – 30 mg/L)			
		Q_{max} (mg/g)	K_L (L/mg)	R^2	n	Q_{max} (mg/g)	K_L (L/mg)	R^2	n
Zeolite	Pb	9.97	0.083	0.985	10	6.54	0.139	0.922	6
	Cu	8.53	0.200	0.937	10	4.34	0.417	0.743	6
	Cd	6.72	0.840	0.992	10	4.20	0.810	0.897	6
	Zn	5.83	0.095	0.985	10	3.72	0.163	0.847	6
	Cr	5.03	0.103	0.990	10	4.01	1.001	0.821	6
ICZ	Pb	11.16	0.157	0.982	10	7.63	0.059	0.938	6
	Cu	9.33	0.095	0.946	10	6.11	0.099	0.780	6
	Cd	7.24	0.110	0.976	10	4.42	0.442	0.951	6
	Zn	6.22	0.095	0.985	10	4.61	0.105	0.859	6
	Cr	5.47	0.092	0.983	10	3.89	0.594	0.932	6

Table 3.

Pseudo-first order and pseudo-second order kinetics models parameters for the adsorption of heavy metals (HM) onto zeolite and ICZ from single metal solutions at pH 6.5 and ionic strength 10^{-3} M $NaNO_3$

Zeolite

HM	Initial conc. (mg/L)	q_e exp.	Pseudo-first order			Pseudo-second order		
			q_e (mg/g)	$k_1 x10^{-2}$ (min^{-1})	R^2	q_e (mg/g)	$k_2 x10^{-2}$ (min^{-1})	R^2
Pb	5.04	4.6	5.39	0.27	0.893	6.17	0.19	0.998
Cu	5.23	4.0	2.90	0.15	0.924	4.61	0.27	0.997
Cd	5.12	4.6	4.57	0.24	0.962	5.32	0.39	0.999
Zn	5.10	4.0	3.25	0.25	0.953	4.54	0.46	0.999
Cr	4.87	2.5	3.15	0.20	0.992	4.04	0.42	1.000

ICZ

HM	Initial conc. (mg/L)	q_e exp.	Pseudo-first order			Pseudo-second order		
			q_e (mg/g)	$k_1 x10^{-2}$ (min^{-1})	R^2	q_e (mg/g)	$k_2 x10^{-2}$ (min^{-1})	R^2
Pb	4.89	5.1	4.08	0.16	0.984	5.29	0.21	1.000
Cu	5.23	4.9	3.05	0.21	0.983	4.92	0.35	0.992
Cd	5.10	4.6	3.79	0.23	0.951	4.13	0.67	0.991
Zn	5.09	4.0	3.22	0.24	0.954	3.96	0.81	0.943
Cr	5.11	3.6	2.01	0.21	0.783	2.56	0.99	0.984

Table 4.

Pseudo-first order and pseudo-second order kinetics models parameters for the adsorption of heavy metals (HM) onto zeolite and ICZ from mixed metal solutions at pH 6.5 and ionic strength 10^{-3}M $NaNO_3$

Zeolite

HM	Initial conc. (mg/L)	q_e exp.	Pseudo-first order			Pseudo-second order		
			q_e (mg/g)	k_1x10^{-2} (min^{-1})	R^2	q_e (mg/g)	k_2x10^{-2} (min^{-1})	R^2
Pb	4.86	4.7	4.32	0.20	0.922	5.57	0.067	0.994
Cu	4.89	3.5	3.14	0.20	0.882	3.61	0.094	0.983
Cd	4.85	3.7	3.45	0.23	0.983	4.30	0.067	0.981
Zn	4.78	3.2	2.88	0.19	0.961	3.96	0.20	0.941
Cr	5.01	2.5	1.51	0.17	0.964	2.42	0.067	1.000

ICZ

HM	Initial conc. (mg/L)	q_e exp.	Pseudo-first order			Pseudo-second order		
			q_e (mg/g)	k_1x10^{-2} (min^{-1})	R^2	q_e (mg/g)	k_2x10^{-2} (min^{-1})	R^2
Pb	5.12	5.0	4.65	0.18	0.972	6.03	0.06	0.994
Cu	5.23	3.7	2.93	0.19	0913	4.18	0.05	0.982
Cd	5.10	4.0	4.38	0.19	0.932	4.81	0.08	0.991
Zn	4.89	4.0	5.41	0.24	0.731	5.36	0.16	0.981
Cr	5.07	3.01	2.84	0.17	0.972	3.55	0.13	0.993

Table 5.

Breakthrough adsorption capacities and Thomas model parameters for column adsorption of heavy metals (HM) from single (pH 6.0) and mixed metals solution (pH 5.0)

		Individual metal				Metals mixture			
	HM	Breakthrough adsorption capacity q_e (mg/g)	q_o (mg/g)	k_{Th} (mL/min.mg)	R^2	Breakthrough adsorption capacity q_e (mg/g)	q_o (mg/g)	k_{Th} (mL/min.mg)	R^2
Zeolite	Pb	1.67	1.61	0.62	0.924	0.63	0.61	1.16	0.899
	Cd	1.32	1.29	0.66	0.894	0.52	0.52	1.06	0.876
	Cu	1.15	1.14	0.88	0.949	0.48	0.49	1.20	0.879
	Zn	1.19	1.10	0.70	0.959	0.45	0.41	1.28	0.917
	Cr	0.81	0.74	1.12	0.945	0.35	0.32	1.72	0.924
ICZ	Pb	2.28	2.03	0.54	0.959	1.03	0.95	1.04	0.954
	Cd	1.89	1.82	0.58	0.933	0.93	0.86	1.08	0.940
	Cu	1.70	1.70	0.66	0.948	0.89	0.83	1.04	0.946
	Zn	1.66	1.61	0.50	0.919	0.83	0.75	1.06	0.933
	Cr	1.17	1.08	0.92	0.949	0.76	0.67	1.14	0.957

Table 6.

Heavy metals adsorption and their desorption by 0.1 M HCl in zeolite and ICZ fixed-bed columns and leaching of Fe during desorption (column height 12 cm, adsorption and desorption flow velocity 0.52 m/h, adsorption after 300 bed volumes, desorption after 40 bed volumes)

Zeolite (Z)								
	1st cycle				2nd cycle			
Metals	Adsorption (mg/g)	Desorption (mg/g)	Desorption (%) *	Fe in leachate (mg/g Z)	Adsorption (mg/g)	Desorption (mg/g)	Desorption (%) *	Fe in leachate (mg/g Z)
Pb	0.63	0.57	90	0.001	0.52	0.44	85	0.001
Cu	0.48	0.31	65	0.001	0.34	0.21	62	0.001
Cd	0.52	0.37	71	0.001	0.37	0.23	62	0.001
Zn	0.45	0.28	62	0.001	0.34	0.21	62	0.001
Cr	0.35	0.23	66	0.001	0.26	0.15	58	0.001

ICZ								
	1st cycle				2nd cycle			
Metals	Adsorption (mg/g)	Desorption (mg/g)	Desorption (%) *	Fe in leachate (mg/g ICZ)	Adsorption (mg/g)	Desorption (mg/g)	Desorption (%) *	Fe in leachate (mg/g ICZ)
Pb	1.03	0.96	93	0.081	0.61	0.52	85	0.006
Cu	0.89	0.69	78	0.081	0.53	0.33	62	0.006
Cd	0.93	0.65	70	0.081	0.54	0.35	65	0.006
Zn	0.83	0.62	75	0.081	0.48	0.33	69	0.006
Cr	0.76	0.49	64	0.081	0.47	0.23	49	0.006

** % desorption = Amount desorbed/Amount adsorbed × 100*

HIGHLIGHTS

- Iron-coated zeolite (ICZ) had higher adsorption than zeolite for Cd, Cr, Cu, Pb, Zn
- Adsorption capacity for Cu, Cd, Zn, Cr decreased at high mixed metals concentration
- Adsorption capacity in batch and column studies: Pb > Cu, Cd > Zn, Cr
- 0.1 M HCl efficiently desorbed metals from ICZ with a small % Fe dissolution
- Data fitted to Langmuir, pseudo-first order, pseudo-second order, and Thomas models